Model-Independent Estimation of the Photokinetic Transfer Matrix from Matrix-Formatted Frequency-Domain Fluorescence

Sharon L. Neal

Department of Chemistry, University of California, Riverside, California 92521

Received: January 10, 1997; In Final Form: April 19, 1997[⊗]

In this paper, the mathematical relationships between matrix-formatted frequency-domain fluorescence decay data and the photokinetic transfer matrix are derived. These relationships reveal that procedures for analyzing the fluorescence spectra and photokinetic mechanism of excited state reactions without model assumptions can be developed when the fluorescence decay is described by first-order differential equations with constant coefficients and when the spectral emission profiles of the decaying fluorophores are distinct. The linear structure of wavelength-dependent frequency-domain decay data permits the simultaneous estimation of the emission spectra, relative initial concentrations, and the photokinetic transfer matrix describing the decay and interaction of multiple fluorophores. Data matrices acquired using a single sample are amenable to this approach, eliminating the necessity to measure probe lifetimes separately at low fluorophore concentration. Most importantly, this method does not require that the analyst choose a kinetic model describing fluorophore emission. Instead, the kinetic mechanism is revealed in the structure of the transfer matrix. Statistical methods can be used to estimate the number of emitting components contributing to a data matrix, so that every aspect of the analysis can be pursued without *a priori* assumptions. Other analytical tools, including a procedure for matrix partitioning to estimate the spectra of sample fluorophores when the spectra are unknown and graphical tools for evaluating prospective spectra and decays, also are described.

Introduction

The similarity of the fluorescence lifetime of many organic molecules and the time scale of molecular motions makes time-dependent fluorescence measurements particularly well-suited for the study of molecular interactions. The wide use of fluorescence probes in a variety of fields including membrane dynamics,[1] protein dynamics,[2] and proton transfer[3] attest to the utility of this approach. Despite this widely used utility, the application of probe methods to investigations of complex systems can be problematic, due to the difficulty in analyzing fluorescence decays especially in the event that excited state reactions occur between probes. The preexponential coefficients and decay constants which characterize a particular decay are typically estimated by using nonlinear least-squares-fitting routines to implement the inverse Laplace transform.[4] Since this transformation is ill-conditioned, measurement errors in the fluorescence signal are inflated, obscuring the number and values of the parameters needed to reconstruct the decay. Moreover, this ambiguity compounds the inherent collinearity of exponential decays (i.e., the similarity of decay profiles even when decay constants differ significantly). Consequently, precise data are required to accurately characterize complex decays, and one is hard pressed to find a multiexponential decay that cannot be described as a combination of three-exponential decays.[5] Given this limitation, decay characterizations utilizing three or more components require external corroboration to establish their physical relevance. This is a central problem in the analysis of the complex decays which are frequently observed for molecules solubilized in microheterogeneous media.

In the case that no excited state reactions occur and component photokinetics are described by a system of coupled first-order linear differential equations, the transfer matrix describing the kinetics between components is a constant, diagonal matrix comprised of the relaxation rates (inverse lifetimes) of the system components. The solution of such a system of kinetic equations consists of monoexponential component decays. The coefficients of the component decays are proportional to the concentrations of the respective components. On the other hand, when excited state reactions occur, the off-diagonal elements of the transfer matrix are nonzero. As a result, the solution of the system of kinetic equations (*i.e.*, the component decays) consists of multiexponential decays whose decay constants are the eigenvalues of the transfer matrix. The preexponential decay coefficients also lose their simple relationship to the initial concentrations because they include terms from the eigenvectors of the transfer matrix. To characterize such a decay, the number of required parameters rises from $2n$ (n decay constants, n initial concentrations) to $n^2 + n$ (n^2 kinetic parameters, n initial concentrations), where n, the number of decaying species, is unknown to the analyst. Typically, the analyst attempts to use the simplest possible model first and incrementally increases the complexity of the model to which the data is fit.[4] Clearly, analyses carried out using this approach are susceptible to biases embedded in the analyst's model choice whether it be from the number of components or in the structure of the transfer matrix (location of zeros). Moreover, the use of fitting routines which are subject to convergence on local minima and sensitive to initial parameter values is an additional source of inaccurate analysis results. The larger the number of fitting parameters, the more serious this limitation is.

As a result of these limitations, efforts to make the analysis of fluorescence decays of systems undergoing excited state reactions less subjective have been reported in the literature regularly. Excimer formation is a very widely studied excited state reaction, and many of these efforts have been directed toward the analysis of excimer decays. The following is a brief history of excimer decay analysis, with a focus on approaches to model-independent analysis. The analysis of excimer decays was pioneered by Birks[6] who described the time evolution of photoexcited pyrene monomers and collisionally excited pyrene

[⊗] Abstract published in *Advance ACS Abstracts,* June 1, 1997.

S1089-5639(97)00170-9 CCC: $14.00

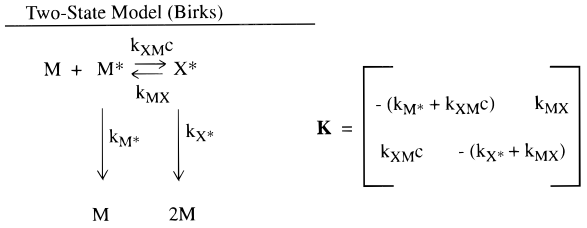

Figure 1. Schematic diagram of Birk's two-state model for excimer formation and its corresponding photokinetic transfer matrix.

excimers using two coupled linear differential equations. A schematic representation and transfer matrix for this model are illustrated in Figure 1. This "two-state" model successfully describes pyrene emission in viscous isotropic liquids and was the basis of many studies correlating the monomer/excimer intensity ratio to the solvent viscosity.[7,8] However, many attempts to apply this model to pyrene decay in hindered and anisotropic media have not been successful.[9,10] In fact, it has been shown that, in many lipid membranes, the dependence of pyrene emission on concentration is inconsistent with diffusion-controlled excimer formation.[11] Consequently, several authors have analyzed fluorescence decays using more complex models. These "three-state" models include a self-quenched pyrene monomer which has other pyrene molecules as near neighbors, but has not formed the excimer proper.[12,13]

Beecham, Ameloot, and Brand showed that the practice of using global compartmental analysis[14,15] to estimate invariant parameters using a series of related measurements also reduced the ambiguity of estimates of excited state reaction parameters, apparently by reducing the range of feasible parameter values. Moreover, because they applied this technique to multidimensional decay surfaces, the emission spectra of the system components were also estimated. However, this method also requires that the analyst select a prospective model and initial parameter values, and then refine the parameter values until the model simulates the experimental data. This approach is therefore subject to the same type of biases, though not to the same degree, as fitting single decays.

Duhamel *et al.*[16] took a totally different approach to the determination of excimer lifetimes. The lifetime of pyrene excimers in sodium dodecyl sulfate micelles was recovered from time domain data without model assumptions. This was accomplished using the constancy of the β-statistic (*i.e.*, a ratio of monomer to excimer decay rates) during the course of the fluorescence measurement to parameterize the excimer lifetime. There are two limitations to this approach that are pertinent to the discussion of model independent analysis. First, the calculation requires that the monomer emission rate be measured separately under different conditions (*i.e.*, low monomer concentration) than those used to produce excimer formation. Second, the statistic was calculated under the assumption that the monomer decay rate is constant across the micelle microdomains, an assumption which other studies refute.[17−19]

Another model-independent analysis is described by Berberan-Santos *et al.*[20] The sum of the system of kinetic equations is a first-order differential equation whose solution is a convolution of the intrinsic decays of all the species participating in a given kinetic mechanism. They estimate the decay constants by fitting experimental data to a convolution of exponential decays in which the decay constants are fitting parameters. This approach is model-independent, but as in the β-method, the analysis does not reveal the kinetic mechanism; it provides access to the excimer decay rate in spite of it. Moreover, the approach requires that the analyst know the number of species participating in the mechanism.

In 1991, Sugar *et al*. presented a clever simplification of excimer lifetime analysis of frequency domain fluorescence data.[21] Until this work, frequency-domain data usually were analyzed using essentially the same approach that is applied to time domain data, by adding an inverse Fourier transform to the inverse Laplace transform. Sugar *et al*. describe pyrene emission in lipids using a three-state model to describe self-quenched monomers, but they did not follow the traditional analysis procedure: (1) simulate the fluorescence impulse (time-domain) response from the model, (2) Fourier transform the impulse response to the frequency domain, and (3) determine the goodness of fit to the experimental data. Instead, they used the identity between the derivative of a function and its Fourier transform to (1) estimate the frequency-domain response directly from the model transfer matrix and (2) measure the goodness of fit. The transfer matrix elements are estimated by minimizing the difference in simulated and experimental data. In the frequency domain, the experimental data are linear functions of the transfer matrix, so that ambiguities reflect measurement errors without inflation due to domain transformations. The primary difficulty in applying the frequency-domain method to experimental data is that it requires accurate measurement of the initial concentrations of the various sample components. These concentrations are unknown when a molecule is partitioning into anisotropic media. Sugar addressed this problem in the case of pyrene-labeled lipids by using statistical mechanics to calculate the relative concentrations of excited state molecules with and without pyrene-labeled lipids as near neighbors. The limitations of this approach are that the analyst is must select the number of emitting species and the structure (number of zeros) of the transfer matrix. Consequently, the approach is subject to the limitations associated with the parameter fitting.

In this paper, the mathematical relationships between matrix-formatted wavelength-dependent frequency-domain fluorescence decay data and the photokinetic transfer matrix are derived. These relationships indicate that procedures for analyzing the fluorescence decays without model assumptions can be developed. These analytical procedures will be applicable to any system which can be described using coupled first-order differential equations with constant coefficients, irrespective of excited state reactions as long as all system components emit luminescence and there is some spectral distinction between them. Emission-frequency-domain fluorescence decay matrices are generated by measuring frequency-domain decays at several emission wavelengths and excitation modulation frequencies. (Of course, the time-domain decays could also be measured as a function of emission wavelength and transformed to the frequency domain.) Emission spectra, modulation ratios, and phase shifts are combined into complex quantum yields[21] and arranged by wavelength into emission-frequency-domain decay matrices. The resultant matrix is then analyzed directly or partitioned into spectral and kinetic factors from which the fluorescence emission spectra of the sample components, their initial excited state concentrations, and the transfer matrix describing the photokinetics of the excited state species can be simultaneously estimated. This partitioning is accomplished by a variation of factor analysis based curve resolution,[22] an approach that has been successfully applied to the resolution of component responses from several types of matrix-formatted spectral data, including steady-state fluorescence data.[23] In the Theory section, the relationship between the emission-frequency-domain decay matrix and the photokinetic transfer matrix, initial excited state concentrations, and emission spectra is derived. In the Analysis section, several tools for analysis of experimental matrices are described. First, rank estimation (*i.e*, the deter-

mination of the number of emitting components) is reviewed. Second, the partitioning of experimental data matrices into spectra and frequency domain decays is described. Finally, graphical approaches to evaluating prospective spectra and decays are described.

The following notation is used throughout this paper. Matrices are denoted by uppercase, boldface Roman and Greek letters; vectors are denoted by lowercase, boldface Roman and Greek letters. Vectors which are columns of a matrix are denoted using the subscripted, boldface matrix variable (*i.e.*, $\mathbf{m}_{\bullet j}$ denotes the jth column of **M**. Similarly, vectors which are rows of the matrix **M**, are denoted $\mathbf{m}_{i\bullet}$, where i represents the ith row. Of course, the matrix element on row i in column j is denoted m_{ij}. Scalars are denoted by lowercase, italic Roman and Greek letters. Complex variables are indicated using a superpositioned tilde (*i.e.*, $\tilde{\mathbf{M}}$). As usual, superscript -1 denotes the matrix inverse, and the slanted prime ($'$) denotes the matrix transpose. Hatch mark (‡) superscripts indicate that the vector or matrix elements have been normalized so that their columns sum to unity.

Theory

Multicomponent Frequency-Domain Decays. The time evolution of many mixtures of n excited fluorophores is described by a system of coupled first-order linear differential equations:

$$d\mathbf{y}/dt = \mathbf{K}\mathbf{y} + \mathbf{f} \tag{1}$$

where **y** is an $n \times 1$ vector describing the instantaneous concentration of the excited fluorophores and **K** is an $n \times n$ transfer matrix whose elements describe the relaxation rates of the components (k_{ii}) and the rate of conversion from one state to the other (k_{ij}). For example, in the two-state model (Figure 1), k_{11} describes the deactivation of the monomer excited state, k_{12} describes the rate of excimer formation from the monomer, k_{21} is the rate at which excimer dissociates to excited state monomer, and k_{22} is the relaxation rate for the excimer. The vector function **f** is the driving or input function which produces the excited state populations. In time-domain experiments, **f** is ideally a Dirac function provided by an infinitely short laser pulse. In frequency-domain experiments, **f** is a sinusoidally amplitude modulated continuous excitation beam.

The solution of the system of equations in time-domain experiments, assuming excitation powers well below saturating intensities, is given by the expression

$$\mathbf{y}_t = \mathbf{W}e^{\mathbf{\Lambda}t}\mathbf{W}^{-1}\mathbf{y}_0 \tag{2}$$

where **W** is a matrix whose columns are the eigenvectors of the matrix **K** (*i.e.*, $\mathbf{KW} = \mathbf{W\Lambda}$), $e^{\mathbf{\Lambda}t}$ is a matrix that has the exponential of the product of the observation time and the eigenvalues of **K** (observed decay constants) on the diagonal, $\mathbf{W}^{-1}$ denotes the inverse of **W** and $\mathbf{y}_0$ is a vector of the initial concentrations of the emitting excited states. Each component of this solution is a combination of the exponential decays defined by **Λ**.

The solution of the system in frequency-domain measurements is given by the expression

$$\mathbf{y}_t = \mathbf{W}\mathbf{M}e^{-i(\omega t\mathbf{I}+\mathbf{\Phi})}\mathbf{W}^{-1}\mathbf{y}_0 \tag{3}$$

where **W**, $\mathbf{W}^{-1}$, and $\mathbf{y}_0$ have the same definitions as above, **M** is a diagonal matrix of signal amplitudes, $m_{ii} = m_{ex}/(\omega^2 + \lambda_i^2)^{1/2}$, and $e^{i\mathbf{\Phi}}$ is a matrix that has the complex phases of the observed signals on the diagonal. The components of this solution are oscillations that are demodulated and phase-shifted relative to the excitation function. This solution is often written using an expression which emphasizes the connection to the impulse response (eq 2):

$$\mathbf{y}_t = \tilde{\mathbf{y}}_\omega e^{-\iota\omega t} \tag{4}$$

where $\tilde{\mathbf{y}}_\omega$ represents the complex Fourier transform coefficients of $\mathbf{y}_t$ at frequency ω.

As Sugar pointed out, the key to frequency-domain analysis is the relationship between a derivative and its Fourier transform. That relationship is

$$d\tilde{\mathbf{y}}/dt = \mathbf{K}\tilde{\mathbf{y}} = \iota\omega\tilde{\mathbf{y}} - \mathbf{y}_0 \tag{5}$$

Rearrangement yields

$$\tilde{\mathbf{y}} = -(\mathbf{K} - \iota\omega\mathbf{I})^{-1}\mathbf{y}_0 \tag{6}$$

which means that at each modulation frequency, the frequency-domain decay coefficients $\tilde{\mathbf{y}}$ are simple algebraic functions of the photokinetics transfer matrix.

Multivariate Frequency-Domain Decays. When the fluorescence emission is observed as a function of emission wavelength and time, the decays can be combined into a single $r \times b$ data matrix **D** where r is the number of emission wavelengths monitored and b is the number of time bins observed. This matrix is the product of the fluorescence emission spectrum and fluorescence decay; it is analogous to the decay described by eq 2. In matrix notation, **D** can be written as follows:

$$\mathbf{D} = \mathbf{X}\mathbf{Y}' = \mathbf{X}\mathbf{W}\mathbf{\Gamma}\mathbf{Z}' \tag{7}$$

where **X** is the $r \times n$ matrix of sample component emission spectra, **Y** is a $b \times n$ matrix of component decay curves, **Γ** is an $n \times n$ diagonal matrix that has the initial condition vector $\mathbf{W}^{-1}\mathbf{y}_0$ along the diagonal, and **Z** is a $b \times n$ matrix of unit decay curves (*i.e.*, $\mathbf{z}_i = e^{-\lambda_i t}$). The spectra (*i.e.*, the columns of **X**) are normalized so that the intensity of each spectrum is proportional to the product of the absorptivity and fluorescence rate constant of the corresponding fluorophore.

Fluorescence decays measured in the frequency domain also depend on the emission wavelength. The result is a complex matrix $\tilde{\mathbf{D}}$ which is the product of the fluorescence emission spectrum and frequency-domain decay. The dimensions of this matrix are $r \times c$ where r is the number of emission wavelengths monitored and c is the number of excitation modulation frequencies observed. This matrix is analogous to the complex decay described by eq 3.

$$\tilde{\mathbf{D}} = \mathbf{X}\tilde{\mathbf{Y}}' = \mathbf{X}\mathbf{W}\mathbf{\Gamma}\tilde{\mathbf{Z}}' \tag{8}$$

where the definitions of **X**, **W**, and **Γ** are the same as above. $\tilde{\mathbf{Y}}$ is the emission-frequency-domain decay matrix. It consists of the frequency-domain decays of the sample components measured at several modulation frequencies. Equation 6 can be expanded and rearranged to

$$\mathbf{K}\tilde{\mathbf{Y}}' = \tilde{\mathbf{Y}}'\tilde{\Omega} - \mathbf{Y}'_0 \tag{9}$$

where $\tilde{\mathbf{Y}}$ and $\mathbf{Y}_0$ are matrices constructed from the values of $\tilde{\mathbf{y}}$ and $\mathbf{y}_0$ measured at all the modulation frequencies (the rows of $\mathbf{Y}_0$ are identical). $\tilde{\Omega}$ is a matrix that has the complex frequencies, $\iota\omega$, along the diagonal. As long as the number of frequencies is greater than the number of emitting sample components, **K** becomes the unknown in an overdetermined system of equations constructed from the complex part of eq 9

and is easily calculated *via* the expression

$$\mathbf{K} = (\tilde{\mathbf{Y}}'\tilde{\Omega})_{\text{imag}}\tilde{\mathbf{Y}}'^{+}_{\text{imag}} \tag{10}$$

in which the subscript image refers to the complex part of the designated matrix and the superscript + denotes the pseudoinverse of the designated matrix. The pseudoinverse[24] of a matrix is used to solve linear systems when the coefficient matrix, here $\tilde{\mathbf{Y}}'$, is singular and has no inverse. Since $(\tilde{\mathbf{Y}}')^{+}\tilde{\mathbf{Y}}' = \mathbf{I}$, the pseudoinverse calculates the minimum norm solution of an infinite number of system solutions. The initial concentrations are calculated from a rearrangement of eq 9:

$$\mathbf{Y}'_0 = \tilde{\mathbf{Y}}'\tilde{\Omega} - \mathbf{K}\tilde{\mathbf{Y}}' \tag{11}$$

Emission Frequency-Domain Decay Matrix Partitioning. When the spectra of the mixture components are known, the frequency-domain decays of those components can be calculated immediately from $\tilde{\mathbf{D}}$:

$$\tilde{\mathbf{Y}}' = \mathbf{X}^{+}\tilde{\mathbf{D}} \tag{12}$$

When the spectra of the mixture components are not known, because the spectrum depends on the fluorophore environment, the spectra, photokinetics matrix, and initial concentrations can still be estimated by factorization of the emission-frequency domain decay matrix. While the spectra and decays which comprise the matrix are unknown, related matrix components are readily calculated. The singular value decomposition partitions $\tilde{\mathbf{D}}$ into the product of three matrices, two of which are linear combinations of the spectra and frequency-domain decays:

$$\tilde{\mathbf{D}} = \tilde{\mathbf{U}}\mathbf{S}\tilde{\mathbf{V}}' = \tilde{\mathbf{U}}\tilde{\mathbf{Q}}' \tag{13}$$

In the absence of measurement errors, $\tilde{\mathbf{U}}$ is the $r \times n$ matrix of column basis vectors (linear combinations of spectra), $\tilde{\mathbf{V}}$ is the $c \times n$ matrix of row basis vectors (linear combinations of the component frequency responses) and $\mathbf{S}$ is an $n \times n$ diagonal matrix whose elements s_{ii} reflect the contribution of the product $\tilde{\mathbf{u}}_{\cdot i}s_{ii}\tilde{\mathbf{v}}'_{\cdot i}$ to the variance of $\tilde{\mathbf{D}}$.

Since the basis vectors $\tilde{\mathbf{U}}$ and $\tilde{\mathbf{Q}}$ are linear combinations of the component spectra and decays, there must be a transformation matrix, $\tilde{\mathbf{\Pi}}$, which converts those orthogonal basis vectors to the physically relevant matrices $\mathbf{X}$ and $\tilde{\mathbf{Y}}$. That is, since

$$\tilde{\mathbf{D}} = \tilde{\mathbf{U}}\tilde{\mathbf{\Pi}}\tilde{\mathbf{\Pi}}^{-1}\tilde{\mathbf{Q}}' \tag{14}$$

there must exist some $\tilde{\mathbf{\Pi}}$ such that $\tilde{\mathbf{U}}\tilde{\mathbf{\Pi}} = \mathbf{X}$ and $\tilde{\mathbf{\Pi}}^{-1}\tilde{\mathbf{Q}}' = \tilde{\mathbf{Y}}'$. Most importantly, the simple algebraic relationship between $\mathbf{K}$ and the frequency-domain decay data described by eq 9 is preserved. As a result, the initial concentration matrix $\mathbf{Y}_0$ and photophysics transfer matrix $\mathbf{K}$ can be calculated directly from $\mathbf{\Pi}^{-1}$ and $\tilde{\mathbf{Q}}$:

$$\mathbf{K} = (\tilde{\mathbf{\Pi}}^{-1}\tilde{\mathbf{Q}}'\tilde{\Omega})_{\text{imag}}(\tilde{\mathbf{\Pi}}^{-1}\tilde{\mathbf{Q}}')^{+}_{\text{imag}} \tag{15}$$

$$\mathbf{Y}_0 = \tilde{\mathbf{\Pi}}^{-1}\tilde{\mathbf{Q}}'\tilde{\Omega} - \mathbf{K}\tilde{\mathbf{\Pi}}^{-1}\tilde{\mathbf{Q}}' \tag{16}$$

This means that, for a given a spectral transformation, $\tilde{\mathbf{\Pi}}$, the corresponding photokinetic matrix is estimated, completely characterizing the kinetic mechanism without *a priori* assumptions by the analyst.

When the spectra fluorescing components are not known, neither are their quantum yields. Equations 8 can be rewritten to include the quantum yields as matrix components rather than spectral normalization factors:

$$\tilde{\mathbf{D}} = \mathbf{X}^{\ddagger}\Phi\mathbf{W}\Gamma\tilde{\mathbf{Z}} = \mathbf{X}\Phi\tilde{\mathbf{Y}} \tag{17}$$

were the matrix Φ is a diagonal matrix comprised of the component quantum yields. When the emission-frequency-domain decay matrix is analyzed without regard to Φ, the results are $\mathbf{X}^{\ddagger}$, $\Phi'\mathbf{K}\Phi^{-1}$, and $\Phi\mathbf{y}_0$. The component decay times are unaffected by Φ, but the rates of excited state reactions (off-diagonal elements of $\mathbf{K}$) will be scaled by various ratios of component quantum yields. The quantum yield matrix Φ can be constructed from literature or experimental values and inverted to adjust $\Phi\mathbf{K}\Phi^{-1}$ and $\Phi\mathbf{y}_0$ prior to further analysis or data interpretation.

One of the implicit limitations of this treatment is that there is no distinction between discrete and distributed decay processes. Since all the molecules decaying in a distributed system emit the same spectrum, the rank of the matrix $\tilde{\mathbf{D}}$ is insufficient to analyze the distribution. In this case, the emission-frequency-domain decay matrix is given by

$$\tilde{\mathbf{D}} = \mathbf{X}\mathbf{G}\mathbf{W}\Gamma\tilde{\mathbf{Z}} = \mathbf{X}\mathbf{G}\tilde{\mathbf{Y}} \tag{18}$$

were the matrix $\mathbf{G}$ is a matrix of ones and zeros which couples related decays to a single-emission spectrum. In this case, the results of frequency-domain analysis are $\mathbf{X}$, $\mathbf{G}\mathbf{K}\mathbf{G}^{+}$, and $\mathbf{G}\mathbf{y}_0$. Since $\mathbf{G}$ sums the elements across the rows of $\mathbf{K}$ or $\mathbf{y}_0$, these values correspond to the mean properties of distributed decays.

Data Analysis

Pseudorank Estimation. The first step in the analysis of matrix-formatted fluorescence data is the determination of the number of fluorophores which give rise to the observed matrix. The rank of a $r \times c$ ideal fluorescence data matrix, the number of basis vectors required to reconstruct the matrix, is the number of fluorophores which emit distinct spectra n. Measurement errors superimposed on the fluorescence signal increase the rank of an experimental data matrix to m, the smaller of the matrix dimensions (*i.e.*, $m = \min(r,c) > n$). In this case, the singular value decomposition of $\tilde{\mathbf{D}}$ is

$$\tilde{\mathbf{D}} = \tilde{\mathbf{U}}\mathbf{S}\tilde{\mathbf{V}}' = \tilde{\mathbf{U}}\tilde{\mathbf{Q}}' \tag{19}$$

where $\tilde{\mathbf{U}}$ now is the $r \times m$ matrix of orthonormal column (spectral) basis vectors, $\tilde{\mathbf{V}}$ is the $c \times m$ matrix of orthonormal row (decay) basis vectors, and $\mathbf{S}$ is an $m \times m$ diagonal matrix whose elements s_{ii} indicate the variance associated with the corresponding product $\tilde{\mathbf{u}}_{\cdot i}s_{ii}\tilde{\mathbf{v}}_{\cdot i}'$ to the total variance of $\tilde{\mathbf{D}}$. The singular vectors and singular values are ordered by magnitude, so that the first matrix component $\tilde{\mathbf{u}}_{\cdot 1}s_{11}\tilde{\mathbf{v}}'_{\cdot 1}$ describes the largest fraction of the variance of $\tilde{\mathbf{D}}$ which can be described by a rank 1 matrix and the last component $\tilde{\mathbf{u}}_{\cdot m}s_{mm}\tilde{\mathbf{v}}'_{\cdot m}$ describes the smallest. The profile of the singular vectors associated with the first component reflects the largest contributors to the variance of $\tilde{\mathbf{D}}$ (*i.e.*, spectral signals) while that of the last reflects the smallest (measurement errors). In the case of high signal-to-noise ratios, the variance associated with the spectral signal is much larger than that associated with the noise and n is clearly reflected in the magnitudes of the singular values s_{ii}. In the case of low signal-to-noise ratios, determination of n can be a difficult problem. The consensus of several indicators is typically used. Methods comparing the variance of the matrix components (*i.e.*, the relative magnitudes of the s_{ii}) are often less effective in this regime. Methods which compare the frequency content of basis vectors[25,26] capitalizing on the predominance of high-frequency signal components in measurement noise generally are more effective.

Emission-Frequency-Domain Decay Matrix Partitioning. When the spectra of the emitting components are not known, the complex quantum yield matrix must be partitioned into spectra and frequency-domain decays (eq 14) prior to model-independent decay analysis. In other words, the values of the elements of a transformation matrix, $\tilde{\mathbf{\Pi}}$, which convert the column basis vectors $\tilde{\mathbf{U}}$ to the component spectra $\mathbf{X}$, and whose inverse transforms the scaled row basis vectors $\tilde{\mathbf{Q}}$ to frequency-domain decays $\tilde{\mathbf{Y}}$, must be determined. Feasible values of $\tilde{\mathbf{\Pi}}$ can be determined by minimizing an objective function which measures the compliance of the estimates of $\mathbf{X}$, $\tilde{\mathbf{Y}}$, $\mathbf{K}$, and $\mathbf{y}_0$ with the mathematical constraints on physically meaningful fluorescence data. Specifically, the component spectra $\mathbf{X}$ and initial concentrations $\mathbf{y}_0$ should be real and nonnegative. The diagonal elements of $\mathbf{K}$ should be real and nonpositive, while the off-diagonal elements should be real and nonnegative and sum to values that are smaller than the magnitudes of the corresponding diagonal elements. The singular vectors will not meet any of these criteria. The objective function should also measure the agreement between the experimental data matrix, $\tilde{\mathbf{D}}$, and data matrices reconstructed using idealized spectra and decays, $\tilde{\mathbf{D}}^*$. Idealized spectra and decays are estimated matrix factors from which inconsistent elements have been deleted. A reconstructed matrix can be computed by using idealyzed matrix factors in the following rearrangement of eqs 8 and 9,

$$\tilde{\mathbf{D}}^* = \mathbf{X}^*(\mathbf{K}^*)^{-1}(\tilde{\mathbf{Y}} - \mathbf{Y}_0^*) \tag{20}$$

where the asterisk indicates deletion of inconsistent values from the matrix. The χ^2 function which measures this agreement is given by the expression

$$\chi^2 = \frac{1}{\nu_{\tilde{\mathrm{D}}}} \sum_{\lambda,\omega} \left(\frac{\tilde{\mathbf{D}}^* - \tilde{\mathbf{D}}}{\sigma_{\tilde{\mathrm{D}}}} \right)^2 \tag{21}$$

where the variable $\sigma_{\tilde{\mathrm{D}}}$ is a matrix comprised of the standard deviation in the complex quantum yield and $\nu_{\tilde{\mathrm{D}}}$ denotes the number of degrees of freedom in the calculation. The normalization of the columns of $\mathbf{X}$, which reflects the relative quantum yields, can be maintained by including constraints on the normalization (the length) of the columns of $\tilde{\mathbf{\Pi}}$.

Feasible values of $\tilde{\mathbf{\Pi}}$ can be determined by minimizing the length of a vector $\mathbf{e}$, whose elements are the squared sums of the inconsistent elements in the estimates of $\mathbf{X}$, $\tilde{\mathbf{Y}}$, $\mathbf{K}$, and $\mathbf{y}_0$. In other words, the elements of $\mathbf{e}$ are the deviations of the estimates of $\mathbf{X}$, $\tilde{\mathbf{Y}}$, $\mathbf{K}$, and $\mathbf{y}_0$ from the mathematical criteria on these quantities. Since the magnitudes of these vectors are very different, the deviations must be scaled so that all the vector components are of similar size. This is accomplished by dividing the deviations by the corresponding matrix norms. The components of $\mathbf{e}$ are listed (without scaling factors) in eq 22 below. They are the negative and imaginary components of $\mathbf{X}$, the negative and imaginary components of $\mathbf{Y}_0$, the positive diagonals of $\mathbf{K}$, the negative off-diagonals of $\mathbf{K}$, the off-diagonal sums of $\mathbf{K}$, which are larger than the corresponding diagonal elements, and the χ^2 between the experimental and reconstructed matrices. The deviations of the lengths of the columns of $\mathbf{\Pi}$ from their target values (unity in the example below) maintains the normalization of the spectra to their respective quantum yields.

$$e(1) = \sum_{ik} (x_{ik} < 0)^2 \qquad e(2) = \sum_{ik} (x_{ik} \in \mathrm{C})^2$$
$$e(3) = \sum_{jk} ((y_0)_{jk} < 0)^2 \qquad e(4) = \sum_{jk} ((y_0)_{jk} \in \mathrm{C})^2$$
$$e(5) = \sum_{k \neq 1} (k_{k \neq 1} < 0)^2 \qquad e(6) = \sum_{l} (k_{ll} > 0)^2 \tag{22}$$
$$e(7) = \sum_{l} ((\sum_{k \neq l} k_{kl}) > -\mathrm{k}_{ll})^2 \qquad e(8) = \chi^2$$
$$e(9{:}8{+}\mathrm{n}) = \sum_{l} (|\mathrm{l}|\tilde{\tau}_{\bullet l}|| - 1)^2$$

where $i = 1{:}r$, $j = 1{:}c$, $k = 1{:}n$, and $l = 1{:}n$ and C represents the field of complex numbers. The length of $\mathbf{e}$ decreases as the size of these deviations decreases. The transformation elements which minimize the length of the objective function vector reconcile the spectral and kinetic factors to the mathematical constraints on spectra, initial concentrations, and transfer matrices. Deviations from sample specific constraints can be included in $\mathbf{e}$ to facilitate the analysis when they are available.

Graphical Evaluation of Postulated Spectra and Decays. One of the tools available to the analyst for evaluating the results of matrix partitioning is graphical analysis. Two types of plots are useful for assessing the quality of the data and the validity of the postulated spectra and decays. The first is a scatter plot of the rows of the complex quantum yield matrix. The elements of the spectral and frequency-domain decay matrices can be considered coordinates of the rows and columns of $\tilde{\mathbf{D}}$, respectively:

$$\tilde{\mathbf{d}}_{i\bullet} = \sum_k x_{ik} \tilde{\mathbf{y}}_{k\bullet} \tag{23}$$

$$\tilde{\mathbf{d}}_{\bullet j} = \sum_k \mathbf{x}_{\bullet k} \tilde{y}_{kj} \tag{24}$$

When the coordinates are normalized to sum to 1 (or $1 + i$ for complex coordinates), graphs of the coordinates lie within $n - 1$ dimensional simplices whose vertices coincide with the coordinates of the spectra and frequency-domain decays. The dispersion of the row coordinates, $x_{ij}^{\ddagger}$, reflects the degree of overlap in the spectra. The dispersion of the column coordinates $\tilde{y}_{kj}^{\ddagger}$ reflects the overlap of the frequency-domain decays. When one of the spectra has a characteristic base line, (*i.e.*, zero intensity at wavelengths which the other components emit) there are rows which are combinations of $n - 1$ decays. The coordinates of these rows fall on a simplex face. When one of the spectra has a characteristic band (*i.e.*, nonzero intensity at wavelengths which the other components do not emit, there are rows which are comprised of a single decay. The coordinates of these rows fall on the vertex of the simplex. The degree of alignment of the row coordinates with the simplex defined by the spectral coordinates can be used to evaluate prospective spectral profiles. Since the frequency-domain decays generally are overlapped irrespective of the kinetics, the column coordinates are rarely significantly dispersed. These relationships are illustrated using an emission-frequency-domain decay matrix that was simulated from digitized spectra and decay profiles generated by the numerical solution of a system of coupled first-order differential equations. The spectra and frequency-domain decays used to simulate the matrix-formatted data are illustrated in Figure 2a,b. The scatter plot of the row coordinates of the calculated emission-frequency-domain matrix are depicted in Figure 2c.

The second graph which is useful in the evaluation of prospective spectra/decay combinations is the Argand plot of the frequency-domain decays. The Argand plot is an x,y plot of the real and imaginary components of the decay at the various modulation frequencies. Sugar has discussed the dependence of the features of the Argand plot on the photokinetic model in detail.[21] The diagrams can confirm several properties of the

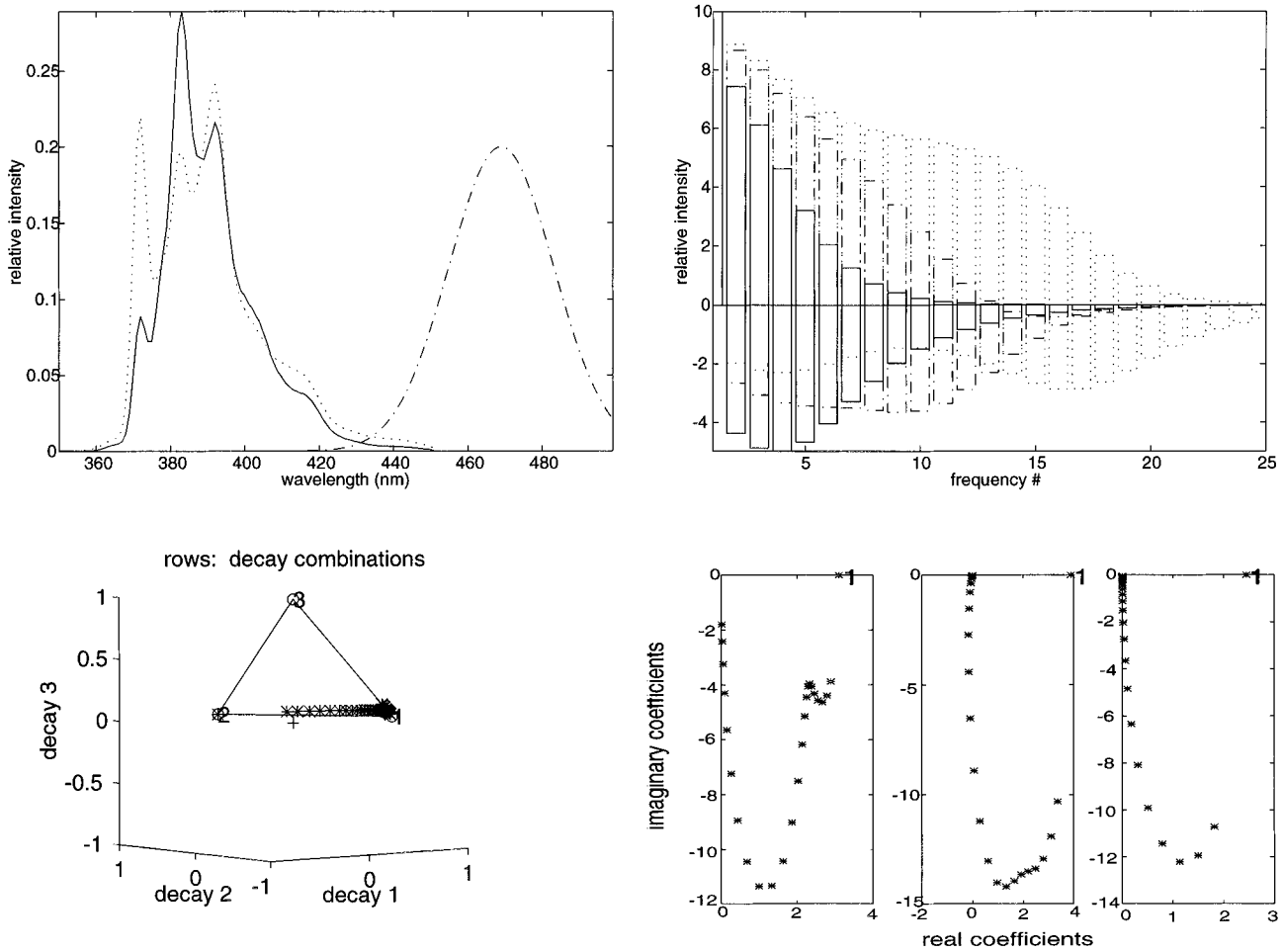

Figure 2. Graphical analysis of simulated emission-frequency-domain decay data. Part a: digitized spectra of the system components. Part b: frequency domain decays of the components. The decays are scaled so that the minor components are visible. Part c: the row coordinate scatter plot. Coordinates on the vertex marked 2 reflect the characteristic wavelengths in the excimer spectrum. Coordinates on the line between vertices 1 and 3 indicate that spectra 1 and 3 overlap at wavelengths which component 2 does not emit. Part d: Argand plots of the unscaled frequency domain decays. The coordinate corresponding to the steady state is marked 1.

photokinetic system: (1) the descriptiveness of coupled first-order differential equations with constant coefficients, (2) the number of fluorescent components, and (3) the mode of fluorophore excitation. The Argand plots of the decays depicted in Figure 2b are illustrated in Figure 2d. They are consistent with undistributed, three-state kinetics with one nonradiatively excited component.

Conclusions

Equations relating the emission-frequency-domain decay matrix to the emission spectra, initial concentrations, and photokinetic transfer matrix of fluorescent mixtures have been derived for systems described by coupled first order differential equations with constant coefficients. When the spectra of the system components are known, the frequency-domain decays of those components, and therefore the photokinetic matrix and initial fluorophore concentrations, can be calculated directly from the emission-frequency-domain decay matrix.[27] When the spectra are not known, the complex quantum yield matrix can be partitioned into spectral and kinetic factors from which the spectra, photokinetic matrix, and initial fluorophore concentrations can be estimated.[28] Several approaches to determining the number of fluorescent components from the data matrix and evaluating the validity of spectra estimated by the partitioning method were reviewed. The construction of a vector valued objective function to direct the partitioning of the complex quantum yield matrix has been described.

Decay analyses based on the relationships described here have several advantages over iterative Laplace transform approaches. The calculations are carried out in the frequency domain, avoiding the inflation of measurement errors that is associated with the transformation process. The simultaneous determination of spectra which correspond to the emitting components supports the physical relevance of the photokinetic mechanism, regardless of how many components are involved. The emission-frequency-domain decay matrix is acquired from a single sample, eliminating the necessity to measure system responses under different experimental conditions. Most importantly, this method does not require that the analyst choose or construct a kinetic model for the fluorophore emission. The structure of the resultant photokinetic transfer matrix reveals the details of the kinetic mechanism.

Acknowledgment. This work was supported by the National Science Foundation (Grants NSF-CHE9314935 and ARI-9313519). The author also thanks the Exxon Educational Foundation for its support during the course of the work described here.

References and Notes

(1) Gennis, R. B. *Biomembranes: Molecular Structure and Function*; Springer-Verlag: New York, 1989; Vol. 1.
(2) Lundblad, J. R.; Laurance, M.; Goodman, R. H. *Mol. Endocrinol.* **1996**, *10*, 607−612.
(3) Waluk, J.; Vogel, E. *J. Phys. Chem.* **1994**, *98*, 4530−4535.

(4) Lakowicz, J. R. *Principles of Fluorescence Spectroscopy*; Plenum Publishing Co.: New York, 1983.
(5) Siemiarczuk, A.; Wagner, B. D.; Ware, W. R. *J. Phys. Chem.* **1990**, *94*, 1661−1666.
(6) Birks, J. B.; Dyson, D. J.; Munro, I. H. *Proc. R. Soc. London, Ser. A* **1963**, *275*, 575−588.
(7) El-Bayoumi, M. A.; Avouris, P.; Kordas, J. *Chem. Phys. Lett.* **1974**, *26*, 373−376.
(8) Vanderkooi, J. M.; Callis, J. B. *Biochemistry* **1974**, *13*, 4000−4006.
(9) Sugar, I. P.; Zeng, J.; Vauhkonen, M.; Somerharju, P.; Chong, P. L.-G. *J. Phys. Chem.* **1991**, *95*, 7516−7523.
(10) Martinho, J. M. G.; Farinha, J. P.; Berberan-Santos, M. N. *J. Chem. Phys.* **1992**, *96*, 8143−8149.
(11) Blackwell, M. F.; Gounaris, K.; Barber, J. *Biochim. Biophys. Acta* **1986**, *858*, 221−234.
(12) Lemmetyinen, H.; Yliperttula, M.; Mikkola, J.; Virtanen, J. A.; Kinnunen, P. K. J. *J. Phys. Chem.* **1989**, *93*, 7170−7175.
(13) Sugar, I. P.; Zeng, J.; Chong, P. L.-G. *J. Phys. Chem.* **1991**, *95*, 7524−7534.
(14) Beechem, J. M.; Ameloot, M.; Brand, L. *Chem. Phys. Lett.* **1985**, *120*, 466−472.
(15) Andriessen, R.; Boens, N.; Ameloot, M.; De Schryver, F. C. *J. Phys. Chem.* **1991**, *95*, 2047−2058.
(16) Duhamel, J.; Yekta, A.; Winnik, M. A. *J. Phys. Chem.* **1993**, *96*, 2759−2763.
(17) Siemiarczuk, A.; Ware, W. R. *Chem. Phys. Lett.* **1990**, *167*, 263−268.
(18) Jay, J.; Johnston, L. J.; Scaiano, J. C. *Chem. Phys. Lett.* **1988**, *148*, 517−522.
(19) Neal, S. L.; Villegas, M. M. *Anal. Chim. Acta* **1995**, *307*, 419−430.
(20) Berberan-Santos, M. N.; Farinha, J. P.; Martinbo, J. M. G.; Duhamel, J.; Winnik, M. A. *Chem. Phys. Lett.* **1992**, *189*, 328−332.
(21) Sugar, I. P. *J. Phys. Chem.* **1991**, *95*, 7508−7515.
(22) Lawton, W. H.; Sylvestre, E. A. *Technometrics* **1971**, *13*, 617−633.
(23) Neal, S. L.; Davidson, E. R.; Warner, I. M. *Anal. Chem.* **1990**, *62*, 658−664.
(24) Strang, G. *Introduction to Applied Mathematics*; Wellesley-Cambridge Press: Wellesley, MA, 1986.
(25) Rossi, T. M.; Warner, I. M. *Anal. Chem.* **1986**, *58*, 810−815.
(26) Shrager, R. I.; Hendley, R. W. *Anal. Chem.* **1982**, *54*, 1147−1152.
(27) Neal, S. L. *Anal. Chem.* **1997**, submitted for publication.
(28) Villegas, M. M.; Neal, S. L. *J. Phys. Chem.* **1997**, *101*.